Open Access

Recent Progress in Materials

LIDSEN Publishing Inc.

Research Article

Non Solved Contemporary Scientific Problems of Non-Conventional Bio-Surfaces Lubrication

Krzysztof Wierzcholski *, Jacek Gospodarczyk

WSG Bydgoszcz University Garbary 2, Bydgoszcz, Poland; E-Mails: Krzysztof.wierzcholski@wp.pl; jacek.gospodarczyk@byd.pl

* **Correspondence:** Krzysztof Wierzcholski; E-Mail: Krzysztof.wierzcholski@wp.pl

Academic Editor: Hossein Hosseinkhani

Special Issue: Non-Conventional Hydrodynamic Lubrication for Biological and Mechanical Surfaces

Recent Progress in Materials
2023, volume 5, issue 1
doi:10.21926/rpm.2301013

Received: December 19, 2022
Accepted: March 06, 2023
Published: March 27, 2023

Abstract

This paper presents new non solved, scientific research directions and their applications in contemporary non-conventional lubrication problems of the bio-surfaces domain. Here are described new research scientific trends and research problem solutions of hydrodynamic lubrication for living tissue, human skin and human cartilage joints surfaces. At first in introduction is described the state of the art, a new purpose of anticipate research and the bio-tribology connections with other scientific domains are documented. The bio-tribology is a new scientific domain where the bio-properties of living, mutually cooperating bio-materials have an important influence on joint human functioning and on the consequences of obtained bio-tribology effects. Using experimental and numerical methods, the main result is focused on the influence of the bio-sweat dynamic viscosity variations across the film thickness on the load carrying capacity of the lubricated human skin and limbs.

Keywords

Living surfaces; lubrication; phospholipid bilayer; human skin; joint cartilage

1. Introduction and Aim of the Research

The bio-tribology knowledge contains experimental and theoretical scientific research of hydrodynamic lubrication, friction and wear at micro- and nano level occurring between mutually cooperating bio-tissues or bio-surfaces of living bodies. The current international level of state-of the-art knowledge of mechanical surface engineering is high today in the field of proceedings conditions on the tribology, fatigue performances, minimum quantity lubrication problems and friction forces connected with abrasive flow [1-6]. The problem of slide bio-bearing and living bio-surfaces lubrication with phospholipids (PL) bilayer, is up today high in the field of chemistry [7-10]. Unfortunately it does not contain unsteady periodic and impulsive hydrodynamic analysis under random dynamic assumptions for deformations of living hyper-elastic cartilage, phospholipid bilayer, human skin surfaces, genetic growth conditions and as an active control in bio-tribology aspects. Moreover, experimental bio-tribology investigation in the nano-sport-medicine and nano-technology field has not been carried out, yet. In the contemporary research of hydrodynamic lubrication problems, mainly the classical constitutive relations for Newtonian synovial fluid flow with constant viscosity in the thin layer liquid lubricant direction, with & without magnetic fields and without hyper-elastic properties of joint cartilage, have been confirmed till now [11-13]. Therefore no existing research will be anticipated in a newly considered bio-nano-tribology and sport-medicine scientific examinations. A new considered investigations will be related to hydrodynamics, theory of elasticity, biomechanics, control systems, sports medicine, physiotherapy, cybernetics, and the theory of vibration, tribology and thetheory of bio-lubrication [14-16]. Thus such models of influences on the living bio-surface lubrication are illustrated in Figure 1. Here are presented three research directions [17, 18]: cyto-bio-tribology, human joint-bio-tribology, his-bio- tribology in nano-medicine and nano-bio-lubrication. New research tendencies are having an important impact on the development of the new scientific domain, which can be called *to-sport-tribology or cito-sport-medicine* for cells, *his-tribology, his-sport-medicine* for tissue in micro and nano level [19-25]. In mentioned scientific domains considered the cooperation between the human skin surface and sports dress during the sport effort. According to contemporary knowledge such scientific domains are completely new and have not been initiated so far by any scientific center and in any sphere of tribology and tissue engineering.

The research undertaken in this work aims to show the influence of the non-Newtonian synovial liquid and human-sweat apparent dynamic viscosity variations across the thin film thickness on the Basal Metabolic Rate (BMR) connected with the human health effects during the lubrication process. In presented research are taken into account the following living, biological regions:

- Inside the superficial living layer of the cartilage tissue sample,
- Between two living phospholipids bilayers,
- Between human skin and tightly fitting dresses,
- Between two cooperating cartilage surfaces in a human joint.

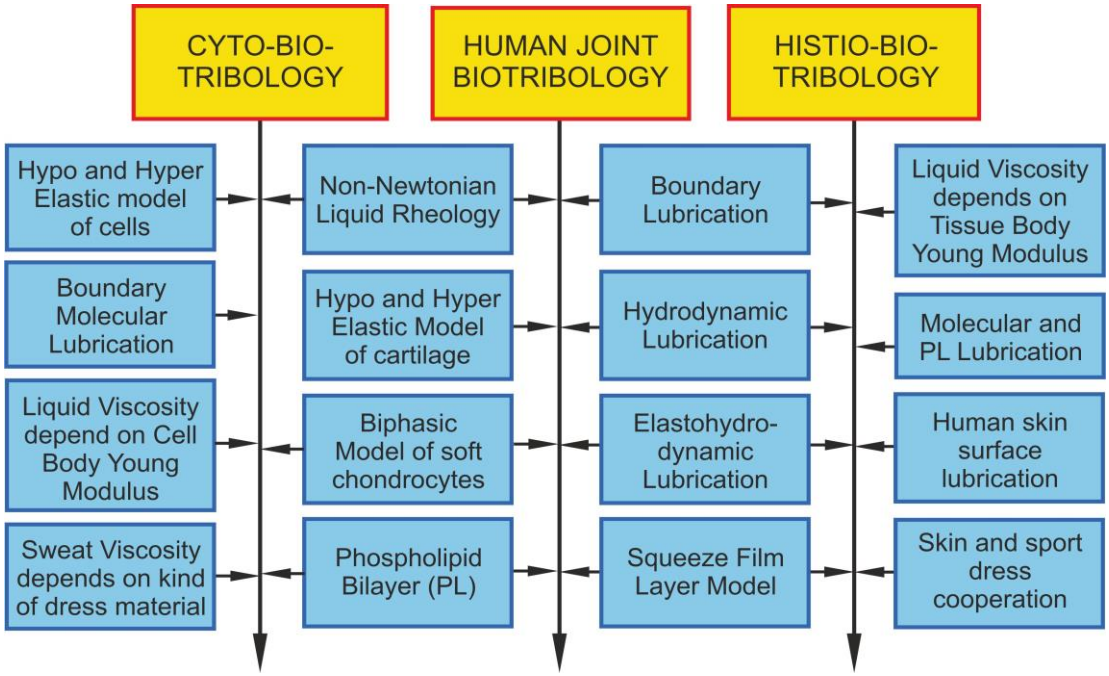

Figure 1 A new scientific aspect research of the lubrication for bio-hydrodynamic contact of cooperating living bio-surfaces in micro and nano- level.

2. Materials, Tools and Methods

2.1 Devices, Tools and Materials for Experimental Methods

In the presented scientific bio-tribology and nano-sport-medicine research, non-living and living materials and anamnesis method were applied. The realization considered examinations had used non-living materials as the following devices: a new generation of Polish Apparatus MF-24, MT-3, and a new German Pulsed Electronic Magnetic Field (PEMF) Magcell Arthro electronic device for the human body, skin and joint cartilage treatment. Moreover had been applied Bone Dias Apparatus produced and constructed by B.Ziegler [15] was used for Acoustic Emission (AE) therapy, Acoustic Sensors, Segmental Body Composition Analyzer Tanita BC 545N, pedometer Garmin Ltd.2015, IKA Viscometer ROTAVISC lo-vi Complete, Atomic Force Microscope (AFM), Scanning Electron Microscope (SEM). The bio-samples of postoperative living materials are gained from PhD.DSc.J. Cwanek, Poland from Rzeszów Technical University. Additionally the living materials and experimental methods had been gained through experience in German research institutes, and practical results were elaborated after measurements and information from students and patients after gymnastic and physical rehabilitation [26-29]. Human sweat had been obtained in laboratory form by way of the pilocarpine iontophoresis using the Gibson-Cook method [30].

2.2 Devices, Tools for Analytical Methods

The theoretical analytical random bio-lubrication problem is described in curvilinear orthogonal coordinates (α_i) situated for i = 1, 2, 3 (in thin gap height direction with I =2) by the stochastic equations of motion, a continuity equation, an energy equation and a Young-Kelvin Laplace equation [31]. Maxwell's equations will be consider the electromagnetic field. The deformations of elastic, hyper-elastic and bio-anisotropic biological bodies, tissues cellular structures of human

joints and skin surfaces are described by the equilibrium of momentum equations, physical dependencies, compatibility equations and the heat transfer equation. We determine expectancy values of the following unknown stochastic functions [31]: hydrodynamic pressure p [Pa], temperature T [K], bio-liquid or fluid velocity components v_i[m/s] for $i = 1, 2, 3$, the dynamic viscosity of synovial fluid $\eta_T(\alpha_1, \alpha_2, \alpha_3)$ [Pas] and the joint gap height ε (α_1, α_3) [m] [31-34]. After term order, the expected function of the bio-liquid or sweat apparent dynamic viscosity η_T[Pa s] has the following form [31]:

$$\eta_T(\alpha_1, \alpha_2, \alpha_3) = \eta_T(n, p_H, We, T, \delta_v, v_0, LA, TA) \quad (1)$$

We denote: k = 1.38054·10^{-23}[J/K]–Boltzmann constant, δ_v– dimensionless collagen fibers concentration in a bio-fluid, ($2 < \delta_v < 6$)**.** The basic equations and Formula (1) show that the dynamic viscosity of the bio-liquid, synovial liquid or sweat is dependent on the dimensionless power hydrogen ion concentration *pH*, wettability *We*[Grade], LA-lactic acid, TA-training activity, U-urea water solution. Non-Newtonian properties are manifested by the dimensionless flow index n whereas (0.8 < n < 1.2). For n = 1, we have Newtonian liquid. Furthermore, we denote: v_0 [m/s] – the characteristic value of bio-liquid velocity. Due to the presence of phospholipids bi-layers on the cartilage surface and liposomes, micelles, macromolecules and lamellar aggregates in the synovial fluid, this liquid has viscoelastic, non-Newtonian especially pseudo-plastic properties [31-35].

2.3 Devices, Tools for Numerical Methods

The main topic of new numerical calculations concerns the Mega-algorithm with UNR (Unit Net Region) for the general and particular numerical solutions of the strong non-linear non-homogeneous partial recurrence equations of the first and second order with variable coefficients occurring in hydrodynamic bio-lubrication of bio surfaces for various curvilinear orthogonal coordinates and for various boundary conditions. A new numerical summation and recurrence methods adjusted to the bio-surface lubrication are presented in the book entitled: Application of The Summation and Recurrence Equations, available on the Lambert Publishing Page [36]. Additionally in this book will be derived the optimization index for the stability of numerical solutions of modified Reynolds Equation, and Poisson Equation with Dirichlet's boundary conditions. Calculation tools such as Matlab 7.3 and Mathcad 15 Professional Programs are implemented.

3. Results for Superficial Bio-liquid Layer Lubrication on the Living Tissue

3.1 Experimental and Numerical Effects

In this section we show the bio-liquid superficial flow and its viscosity in various places of the sample, inside a thin region restricted between the potential flow and superficial layer of tissue in Figures 2a, b, and with phospholipid (PL) bilayer coated by the hydrated sodium ions in Figures 3a, b. The mentioned gap is filled with the physiological liquid boundary. The variable velocity components v_x,v_z in two directions x and z and the corresponding variable bio-liquid dynamic viscosity across the gap height is presented in Figures 2a, 3a. The height of the layer region is presented in Figures 2b, 3b. The bio-liquid with flow rate Q_0 is delivered into a superficial layer in both samples presented in Figures 2b and 3b.

The velocity and dynamic viscosity distribution values depicted in Figures 2a, 3a are obtained after numerical calculations using the summation and recurrence method [36, 37] and AFM measurements using IKA Viscometer ROTAVISC lO-vi Complete. The values obtained in a thin film using the measurement method are similar to those calculated by the numerical method presented in [31] https://www.lidsen.com/journals/rpm/rpm-03-02-023. In this experiment are used following data values are the Wettability of phospholipid bilayer We = 60°, power hydrogen ion concentration in bio-liquid pH = 8, dimensionless coefficient of collagen fibers concentration in bio-liquid δ_v = 4, dimensional collagen fibers concentration c_c = 50,000 mol/mm^3, non-Newtonian bio-liquid flow index n = 0.9. We can see that the smallest liquid flow velocity values are assigned to the larges liquid dynamic viscosity values. The largest liquid flow velocity values correspond with the smallest values of liquid dynamic viscosity [38].

Up to now in scientific papers, describing non-isothermal hydrodynamic bio-lubrication problems, many Authors had been neglected the bio-liquid viscosity variations in gap height direction [7, 10, 15, 24, 38]. Such assumptions were considered by the statement of very small temperature differences in bearing gap height direction. However, the contemporary AFM measurements of physiological-liquid flows in a thin layer require taking into account the variations of the bio-liquid dynamic viscosity across the thin layer [31, 38]. The adhesion forces cause mentioned variations, wettability of the phospholipid bilayer restricted the gap, hydrogen ion concentration (pH) in bio-liquid, shear rate and velocity during the flow and temperature gradients [38].

To the author's knowledge, contemporary scientific effort in the bio-tribology domain, usually does not contains the possibility to consider the measurements of bio-liquid viscosity in the interval from 1.0 mPas (cP) to 5.0 mPas (cP), because it is very difficult to measure mentioned thin gaps height values from 10 nm to 10 µm [10, 12, 15]. This statement refers to the tribology interpretation, for periodic and impulsive hydrodynamic analysis under various non-conventional deformations of hyper-elastic cartilage surfaces, and genetic growth conditions as well an active control in bio-tribology aspects. Experimental bio-tribology investigation in the bio-nano-technology field, connected with measurements of thin liquid dynamic viscosity across the lubricant thickness, had been seldom carried out [39]. Hence the semi-numerical analysis of the dynamic viscosity variations across the thin bio-liquid superficial layer has an important meaning.

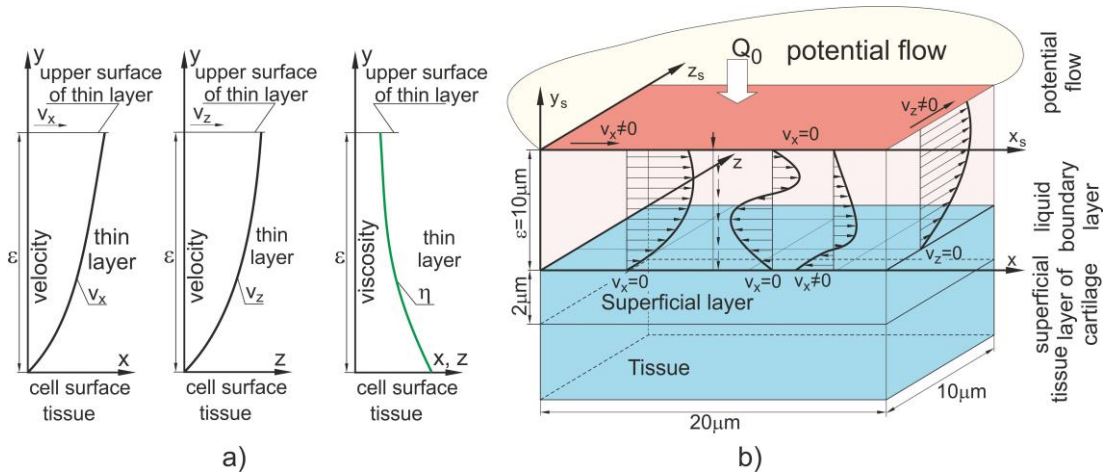

Figure 2 Bio-liquid velocity and dynamic viscosity distributions across the thin bio-liquid boundary layer, during the cartilage-surface pouring lubrication with flow rate [Q_0] = 20 $\mu m^3/s$: a)velocity [v] = 0.02 m/s and corresponding dynamic viscosity distributions [η] = 0.04 Pas flow surface in temperature T = 310 K, b) micro-level illustration of the thin liquid boundary layer restricted by the superficial cartilage layer and movable potential flow.

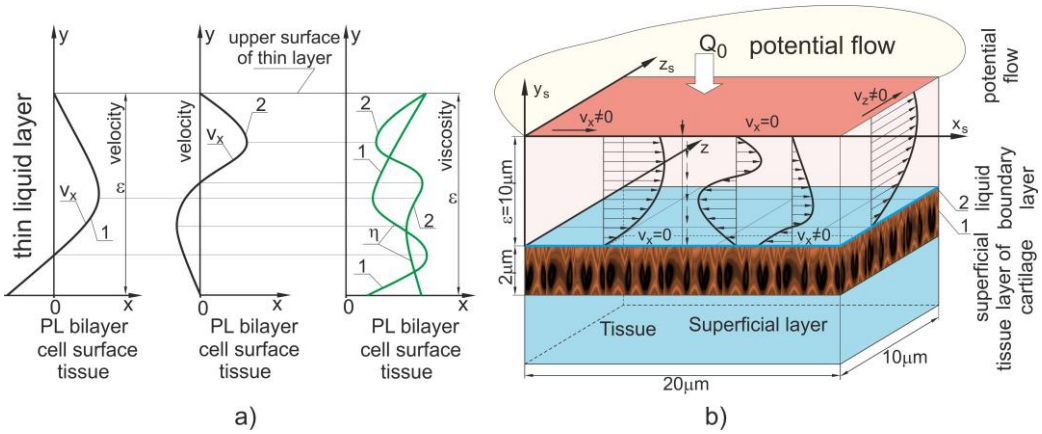

Figure 3 Bio-liquid velocity and dynamic viscosity distributions across the thin bio-liquid boundary layer, during pouring lubrication cartilage with flow rate [Q_0] = 30 $\mu m^3/s$: a)velocity [v] = 0.03 m/s and corresponding dynamic viscosity distributions [η] = 0.04 Pas and in temperature T = 310 K, b) micro-level illustration of the thin Liquid boundary layer restricted by the potential flow and cartilage coated by the phospholipid bilayer 1 and hydrate sodium ions 2.

4. Results for Thin Bio-liquid Layer Lubrication between Phospholipids Bilayer

4.1 Phenomenon of Phospholipid Bilayer Lubrication

In this section, by numerical calculations, we show the phenomenon of the bio-lubricant dynamic viscosity variations across the very thin bio-liquid layer. Presented in the next intersection Figures 4, 5, 6, 7, 8 show the gap filled by the thin (ε= 12 micrometer height) physiological lubricant layer, restricted by the two cooperating phospholipid (PL) bilayer. Numerical calculations are performed using UNR-Mega Algorithm [36] for: Wettability We = 60°, pH = 6, the concentration of collagen fibers δ_v = 4, bio-liquid flow index n = 0.9. In this flow we have: dimensional collagen fibers

concentration c_c = 50 000 mol/mm^3, flow without electrostatic intensity E = 0 V/m, interfacial energy γ = 3.0 mJ/m^2, iso-electrical point IP γ = 3.5 mJ/m^2. After experimental measurements applying the Atomic Force Microscope, using Viscometer ROTAVISC lo-vi Complete and considering numerical analysis [34, 38] follows, that the flow velocity component v_x presented in Figures 4, 5, 6ab, 7ab, 8ab, and bio-liquid dynamic viscosity distributions η across the gap height (Figures 6c, 7c, 8c) are not constant. The final velocity distribution values obtained across the gap height in sections A, and B presented on the left side of Figures 4, 5, 6c, 7c, 8c, are assigned to the values of dynamic viscosity distribution η in the gap height direction, depicted on the right-hand side of the mentioned figures. We can see that the dynamic viscosity distribution in thin gap height direction, depends on the variations of velocity and shear rate distribution [39]. In Figures 4, 5, 6, 7, 8 the pressure quantity p is of order O (0.150 MPa) with temperature values 310 K < T < 312 K. Decrements of the flow velocity and shear rate values imply the liquid dynamic viscosity increases from 0.003 Pas to 0.300 Pas. We can see that the places of maximum (minimum) velocity in the thin layer height physiological liquid direction, have the minimum (maximum) values of the liquid dynamic viscosity. However, if velocity attains values in zero neighborhood, then the viscosity tends only to approximate value 0.300 Pas, on the ground of measurements. We obtain similar results (but with differences of about 3%) applying the measurements using the shear ultrasonic reflection method [40].

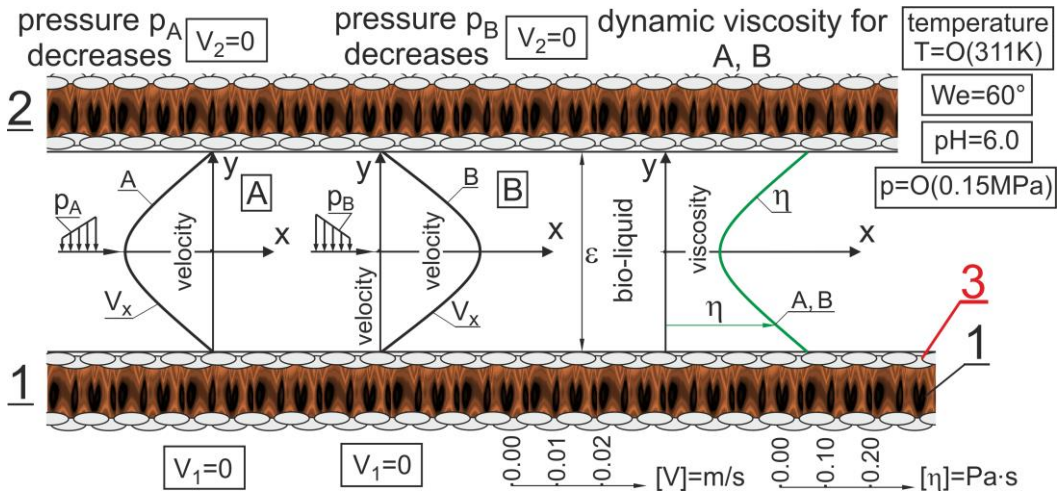

Figure 4 Determination of the dynamic viscosity η distribution across the thin bio-liquid boundary layer in two sections A&B between motionless lower (1) and upper (2) phospholipid bilayer coated with the hydrate sodium ions 3 and loaded with the pressure increasing in section A, and pressure decreasing in section B. Notations: velocity component v_x with values V_1, V_2 equal to zero on the lower and upper PL bilayer.

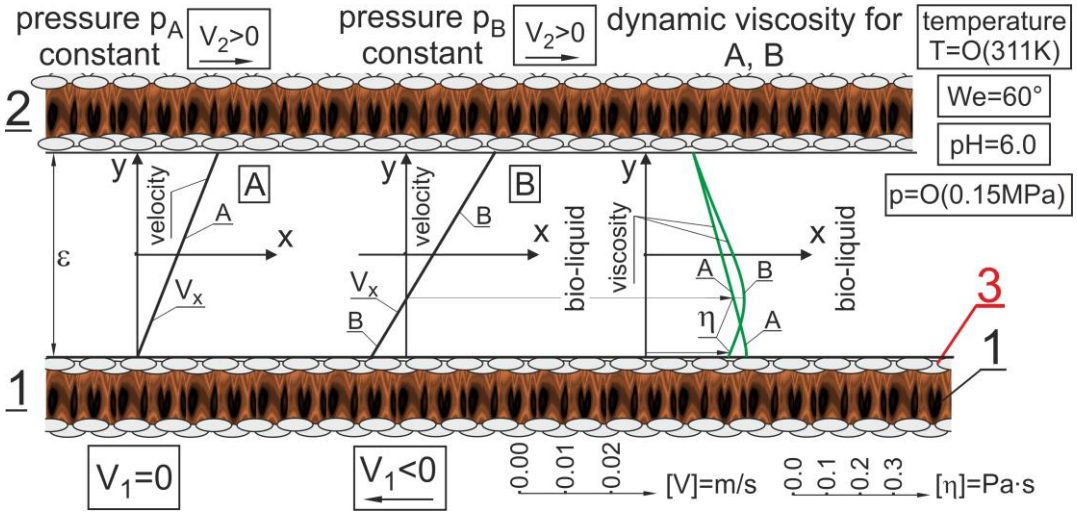

Figure 5 Determination of the dynamic viscosity η distribution across the thin bio-liquid boundary layer in two sections A&B, between movable upper (2) PL surface and motionless lower surface in section A, and between movable upper surface (2) and movable lower surface (1) in opposite directions in section B, coated with the hydrate sodium ions 3 whereas both sections A and B are loaded with the constant pressure values. Notations: velocity component v_x with values V_1, V_2 on the lower and, upper PL bilayer.

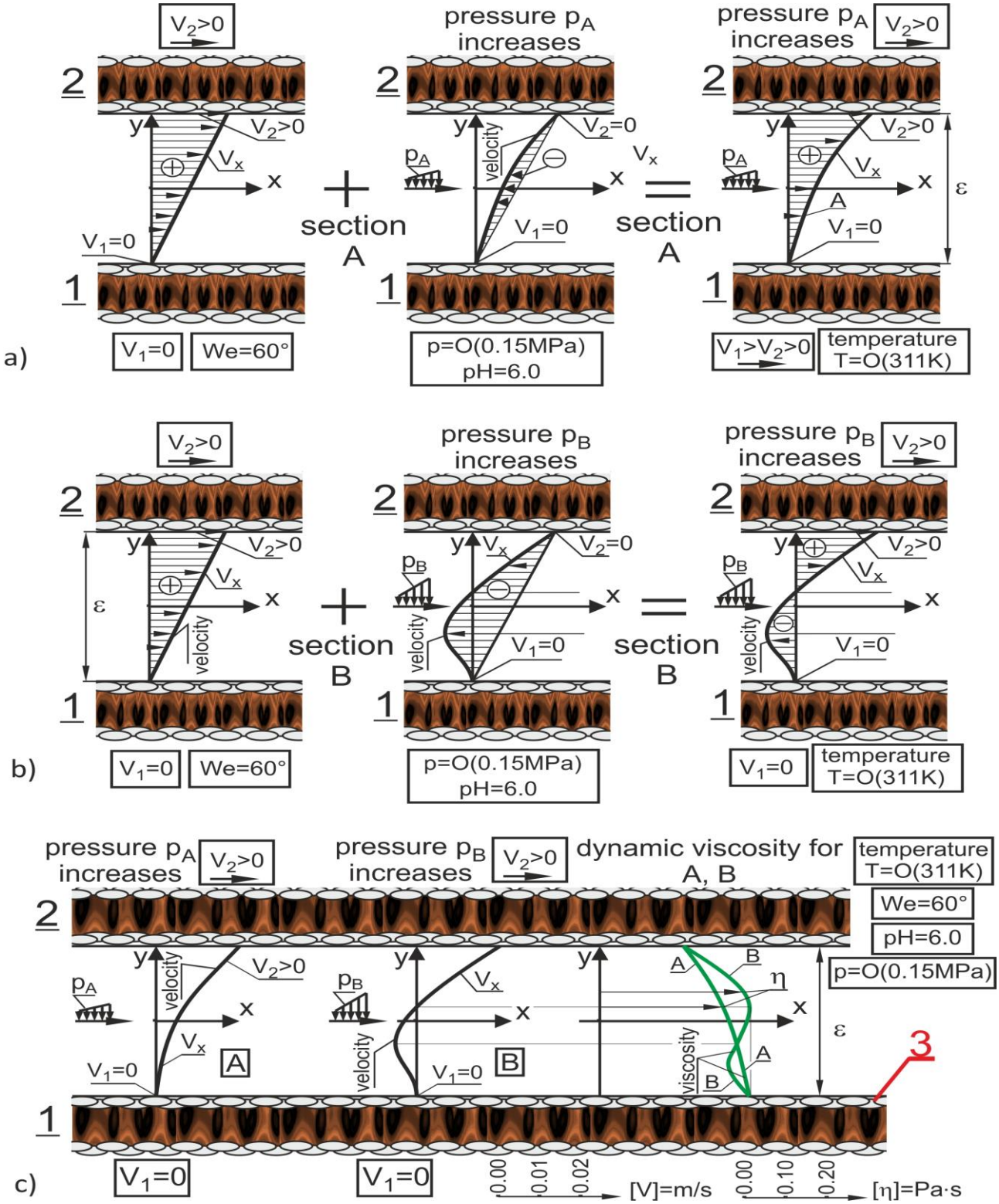

Figure 6 Dynamic viscosity η distribution across the thin bio-liquid boundary layer, for the flow between motionless lower (1) and movable upper (2) PL surface: a) loaded by the small increasing of pressure p_A in section A, b) loaded by the large increasing of pressure p_B in section B, c) Assignations of the flow velocity values in A and B to the dynamic viscosity values η. Notations: Positive values V_1, V_2 of velocity component v_x presented on the lower and upper PL bilayer coated with the hydrate sodium ions 3.

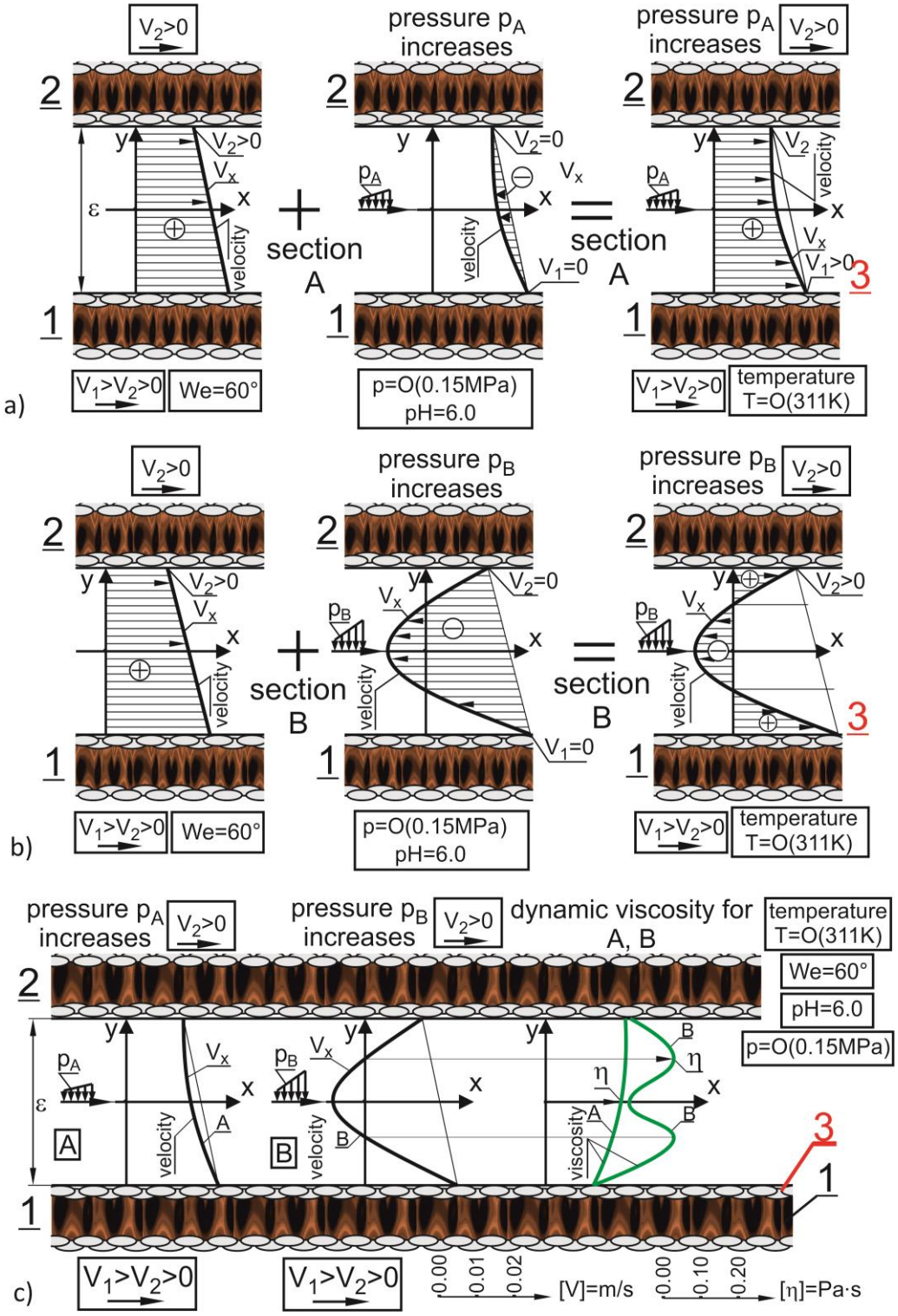

Figure 7 Determination of the dynamic viscosity η distribution across the thin bio-liquid boundary layer for the flow between movable lower (1) and upper (2) phospholipid surface: a) loaded by the small increasing of pressure p_A in section A, b) loaded by the large increasing of pressure p_B in section B, c) Assignations of the flow velocity values to the dynamic viscosity values η. Notations: bio-liquid velocity component v_x with positive values $V_1 > V_2$ on the lower and upper PL bilayer coated with the hydrate sodium ions 3.

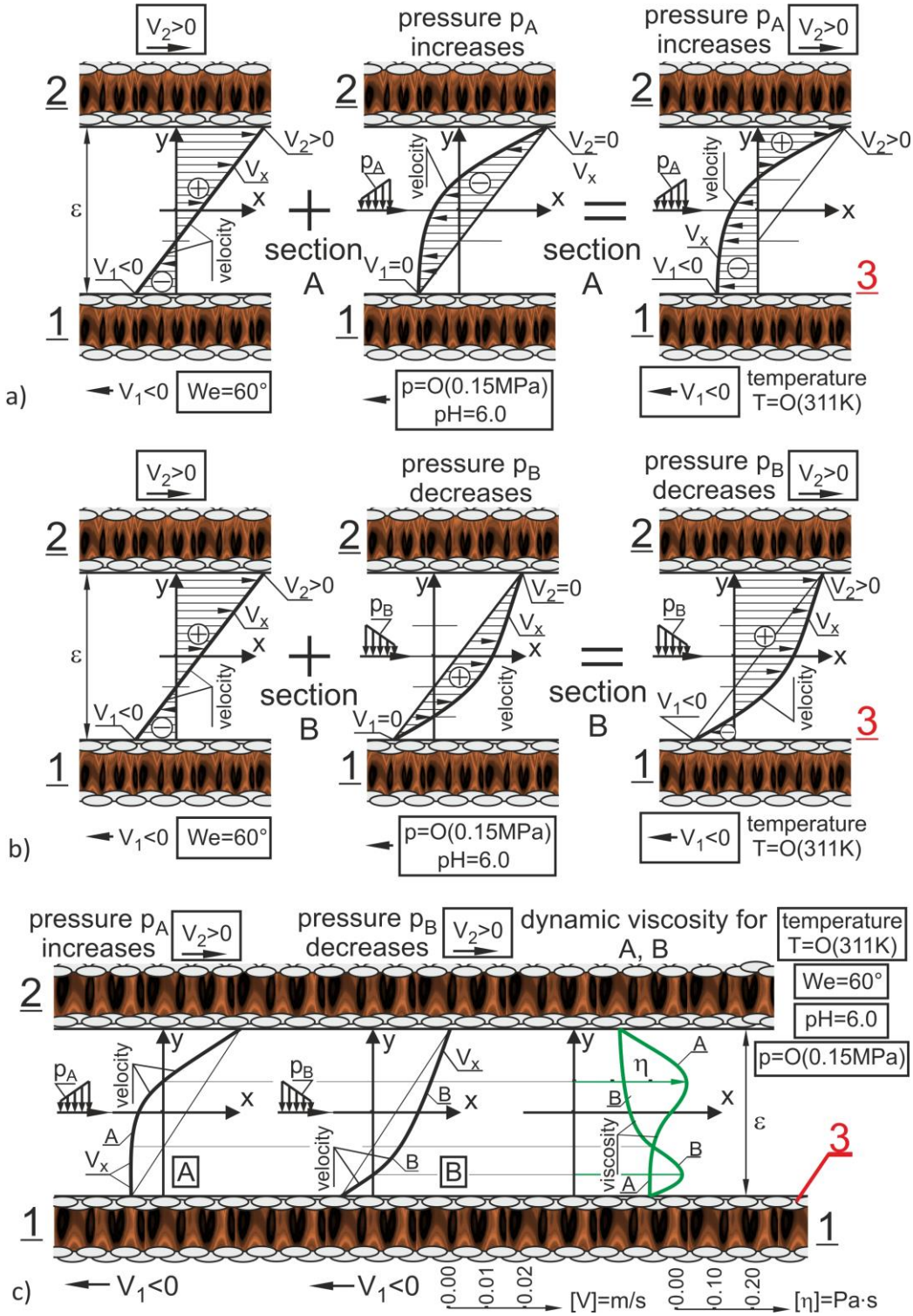

Figure 8 Determination of the dynamic viscosity η distribution across the thin bio-liquid boundary layer for the flow between lower (1) and upper (2) phospholipid surface movable in opposite directions: a) loaded with the pressure increasing p_A in section A, b) loaded with the pressure decreasing p_B in section B, c) Assignations of the velocity values to the dynamic viscosity values η. Notations: bio-liquid velocity component v_x with absolute values $V_1 > V_2$ on the lower and upper PL bilayer, coated with the hydrate sodium ions 3.

4.2 Numerical and Experimental Effects for Phospholipid Bilayer Lubrication

In Figure 4 section A, we can see that the hydrodynamic pressure increases in a positive direction; hence we have the liquid flow distribution in a negative direction, i.e., back-liquid flow. And in section B the hydrodynamic pressure decreases in a positive direction. Hence we have the bio-liquid flow distribution in a positive direction. Upper and lower PL surfaces are motionless. Thus the velocities V_1, V_2 of the lubricant liquid particles directly in contact with the internal PL surfaces, have a zero value. Figure 4 shows, that the bio-liquid lubricating flow inside the thin layer between two phospholipid bilayer is generated only by the values of hydrodynamic pressure variations, i.e., increases in section A and decreases in section B [33, 39].

Figure 5 shows, that the constant hydrodynamic pressure does not generate the bio-liquid lubricating flow inside the thin layer between (2) two PL bilayer. And flow is generated only by the motion in two opposite directions of the lower and upper PL surfaces [33, 39].

The coinciding point of two charts, A and B, of dynamic viscosity in Figure 5 denotes the point in gap height direction with identical absolute velocity values in sections A and B.

Figures 6a, b show, that the lubricant parabolic flow distribution in the negative direction inside the thin layer between (2) two PL bilayer in sections A and B is generated by the hydrodynamic pressure increases in a positive direction [33, 39]. And simultaneously the motion of the upper PL surface in a positive direction implies the flow in a positive direction. In contrast, the, lower surface is motionless in sections A and B.

In Figure 6a and 6b the velocities of the lubricant liquid particles directly in contact with the lower internal PL surfaces, have values zero $V_1 = 0$ and particles directly in contact with the upper internal PL surface have value $V_2 > 0$, equal to the upper surface velocity. The final value of liquid flow velocity distribution in gap height direction presented in Figure6a and 6b illustrates the difference of velocity triangle distribution in positive direction caused by the PL surface motion and parabolic velocity distribution in negative direction generated by the hydrodynamic pressure [33, 39].

Figure 6c on the left hand side, assigns the final velocity values obtained in Figure6ab to the corresponding dynamic viscosity values on the right hand side. Moreover, the point in gap height direction with identical values of velocity distribution in section A and B has the same dynamic viscosity value. Thus two charts A, B of dynamic viscosity have coinciding point [33, 39].

Figure 7a and 7b show, that the parabolic lubricant flow in a negative direction, inside the thin layer between two PL bilayer is generated by the hydrodynamic pressure increasing in a positive direction, whereas mentioned pressure increasing in sector B is larger than increasing in sector A [33, 39].

The flow presented in Figure 7c is generated simultaneously by the motion of the upper and lower PL surfaces both in a positive direction. In contrast, the, lower the surface moves larger than upper surface, i.e., $V_1 > V_2$. Thus the velocities of the lubricant liquid particles contacting directly with the lower and upper internal PL surfaces, have both not zero values equal to the proper surface velocity.

The final value of liquid flow velocity distribution in gap height direction presented in Figure 7a and 7b illustrates the difference of velocity trapezoid distribution in a positive direction caused by the lower and upper PL surface motion in a positive direction and parabolic velocity distribution in a negative direction generated by the hydrodynamic pressure increases in a positive direction [33, 39]. Figure 7c assigns the final velocity values obtained in Figure 7a and 7b to the corresponding

dynamic viscosity values. The dynamic viscosity on the lower surface is smaller than the dynamic viscosity on the upper surface, because the positive value of velocity V_1 on the lower surface is larger than the positive velocity value V_2 on the upper surface.

Figure 8a shows in section A, that the parabolic lubricant flow in a negative direction, inside the thin layer between two PL bilayer is generated by the hydrodynamic pressure increasing in a positive direction, and simultaneously by the motion of the upper PL surfaces in positive direction and lower surface in negative direction [33, 39].

Figure 8b shows in section B, that the parabolic lubricant flow in a positive direction, inside the thin layer between two PL bilayer is generated by the hydrodynamic pressure decreasing in a positive direction, and simultaneously by the motion of the upper PL surfaces in a positive direction and lower surface in negative direction [33, 39].

Thus in sections A and B the velocities of the lubricant liquid particles directly in contact with the internal PL surfaces, have positive values $V_2 > 0$ in the upper and negative values $V_1 < 0$ in the lower surface.

The final value of liquid flow velocity distribution in gap height direction presented in Figures 8a and 8b sections A, and B illustrates the sum of two-triangle positive and negative velocity distribution caused by the lower and upper PL surface motion in two opposite directions and parabolic velocity distribution in as negative direction in section A (positive direction in section B) generated by the hydrodynamic pressure increases in a positive direction (in section A) and pressure decreases in a positive direction (section B).

Figure 8c assigns the final velocity values obtained in Figures 8ab to the corresponding dynamic viscosity values. The dynamic viscosity on the lower surface is larger than the dynamic viscosity on the upper surface, because the absolute value of velocity V_1 on the lower surface is smaller than the positive velocity value V_2 on the upper surface. The coinciding point of two charts, A and B, of dynamic viscosity in Figure 8c is assigned to the point with the same lubricant velocity values in the gap height direction presented in sections A and B [33, 39].

5. Results for Thin Sweat Layer Lubrication between Human Skin and Tightly Fitting Dress Surface

5.1 Phenomenon of Human Skin Lubrication

This intersection has presented the phenomenon of the hydrodynamic sweat lubrication in the thin gap between the movable external human skin surface and leggings or tightly fitting gymnastic dress surface. Total skin of sound human excrete (eliminate) usually about 1200 ml sweat daily and after intensive gymnastic training additionally 700 ml sweat. European human sweat is mostly (93 percent) water, electrolytes, fatty acids, lactic acid, and nitrogen metabolites, such as ammonia, urea, and uric acid [30, 41]. The trace amounts of minerals, lactic acid, and urea are dissolved in the water. Urea –water-solution (UWS) is calculated based on experimental and literature data and has dynamic viscosity value equal from 1.36 to 1.63 mPas (cP) in temperature 293 K. And alone lactic acid dynamic viscosity can even attain a value of 18 mPas [42, 43]. Power hydrogen ion concentration (pH) for European human sweat attains values from 4.2 to 7.5 [30]. Some concentration of minerals is: sodium (from 0.8 to 0.9 g/l), potassium (from 0.1 to 0.2 g/l), and calcium (0.0015 g/l). Sweat density in temperature 293 K is 0.998 to 1.012 g/cm^3. After performing own measurements using Viscometer ROTAVISC lo-vi Complete, and calculations from equation (1) based on the literature data [44, 45], the dynamic viscosity η of typical human sweat has values in

the interval from 1.21 to 4.02 mPas. On the ground of the Authors' knowledge abovementioned data is non-valid for African and Asiatic human.

Figures 9, 10, 11, 12 presented in the next intersections, are graphically presented the mutually connections between viscosity η and lactic acid sweat component LA, training activity TA, power hydrogen ion concentration pH, and wettability We values of the dress surface.

5.2 The Numerical and Experimental Effects for Human Skin Lubrication

Figure 9 illustrates the sweat viscosity increments if lactic acid increases. Lactic Acid LA increments are connected simultaneously with the Training Activity TA increases. After the author's calculations and laboratory measurements [30] follows, that the increments of lactic acid (LA) and TA, increases the dynamic sweat viscosity η see Figure 9. This fact denotes that the increments of TA lead to the sweat dynamic viscosity increases and consequently implies the load carrying capacity increments. Thus after an individual inquires about anamnesis from 20 athletes, the runner easier defeats the body inertia forces of air resistance during the run. For the Training Activity Effort TA, we initiate conventionally unit [level] from 1 to 5. As a one unit we understand the sportsman's effort for the run of 100 m with a velocity of 2 m/s. Hence, the unit level 5 denotes the effort during the run at a distance 500 m with the speed 2 m/s. During the increments of intensive training activity TA in level effort from 1 to 5, the hundred milliliters of human sweat includes an average from 100 mg to 450 mg lactic acid (LA) component. After very intensive training, human sweat's lactic acid (LA) component can seldom attain even 1700 mg in 100 ml of sweat [30, 43, 44]. LA dynamic viscosity decreases with temperature increments.

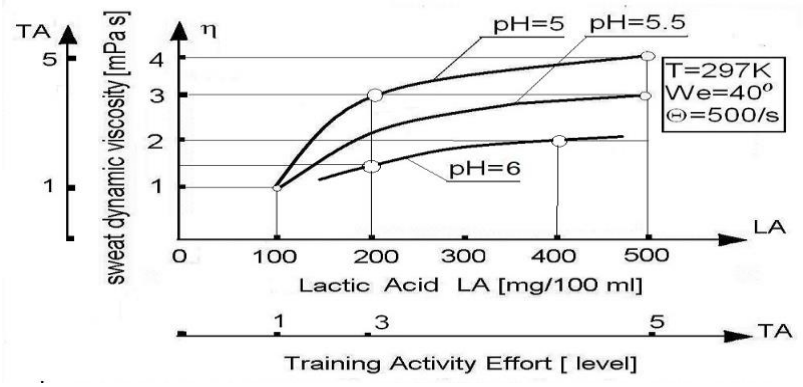

Figure 9 Increments of the sweat dynamic viscosity η in [mPas] versus increases of the lactic acid LA from 100 to 500 mg/100 ml sweat, for various dimensionless values of power hydrogen ion concentration pH, constant temperature value T = 297 K, and constant shear rate value Θ = 500/s of sweat flow, constant value of dress material wettability We = 40°

Figure 10 shows that human sweat power hydrogen ion concentration pH from 4.0 to 7.9 [30, 43, 44]. Analogously to the considered dynamic viscosity variations versus pH for physiological liquids [34], we can conclude, that the dynamic viscosity η of human sweat decreases if the $4 < pH < 8$ increases. Figure 10 shows that the small values of training activity efforts TA, denote large values of the sweat power hydrogen ion concentrations pH. And the large values of training activity efforts TA, denote small values of the sweat power hydrogen ion concentrations pH. Hence during the

increments of sport training activity TA, the sweat's pH decreases and, consequently, sweat dynamic viscosity η increases [30, 43, 44].

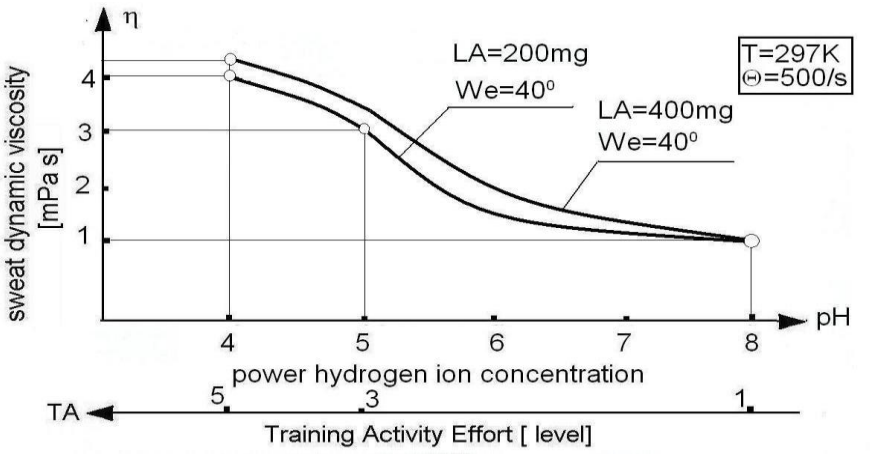

Figure 10 Decrements of the sweat dynamic viscosity η in [mPas] versus dimensionless values of power hydrogen ion concentration pH increases for various values of lactic acid LA = 200,400 mg/100 ml sweat, and constant temperature value T = 297 K, and constant shear rate value Θ = 500/s of sweat flow, constant value of dress surface wettability We = 40°.

Figure 11 illustrates the lactic acid LA increments versus simultaneous increases of training activity TA and sweat dynamic viscosity η increases. Men sweat of European includes more lactic acid (LA) than women's [29, 43, 44]. Thus by the laboratory measurement results following [43, 44], the power hydrogen ion concentration pH for man sweat is smaller than the pH of woman sweat. Hence by the above mentioned remarks due to viscosity versus pH, it follows, that the man's dynamic sweat viscosity η is larger than dynamic viscosity of woman's sweat.

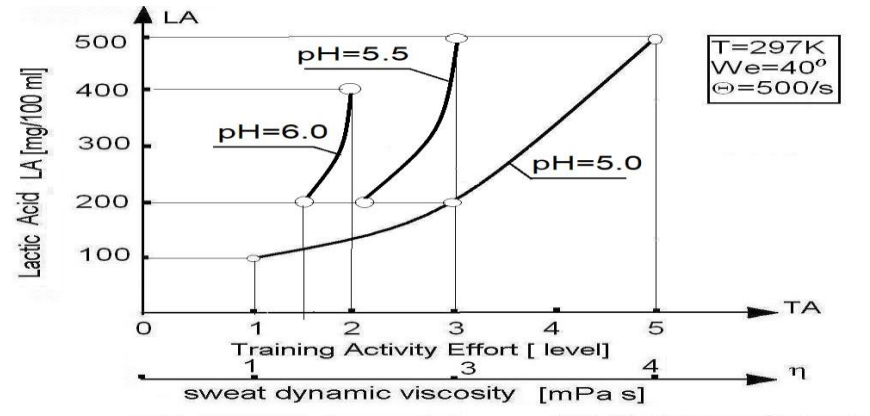

Figure 11 Increment of average values of lactic acid LA = 100-500 mg/100 ml sweat, versus increases of training activity efforts in [level = 1, 2, ...] for various dimensionless values of power hydrogen ion concentration pH from 4 to 6, constant temperature value T = 297 K, and constant shear rate value Θ = 500/s of sweat flow, constant value of dress surface wettability We = 40°.

Figure 12 illustrates the power hydrogen ion concentration decrements versus simultaneously increases of training activity TA and sweat dynamic viscosity η increases.

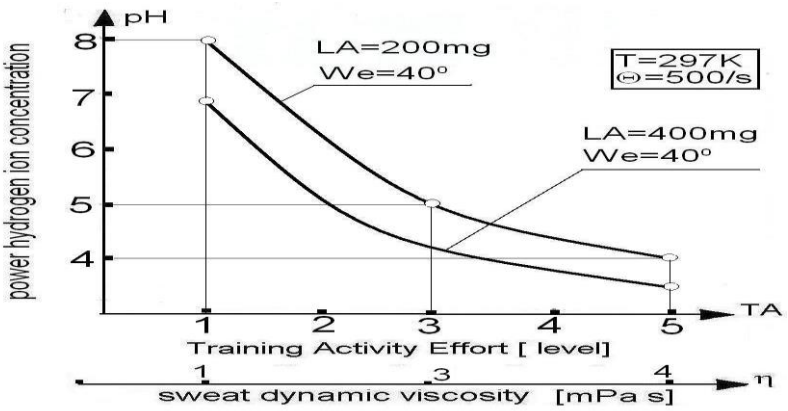

Figure 12 Decrement of dimensionless hydrogen ion concentration values pH versus increases of training activity efforts in [level 1, 2, …] for constant value of dress surface wettability We=40 grad, and various values of lactic acid values LA = 200,400 mg/100 ml sweat], constant temperature value T = 297 K, constant shear rate value Θ = 500/s of sweat flow.

Figures 9-12 be labeled as Figure 13. Here the gap filled by the thin (ε = 5 micrometer height) layer is presented, restricted by the mutually cooperating human skin and the internal surface of sport dress material. After experimental measurements applying the Atomic Force Microscope and numerical analysis using UNR-Mega Algorithm [36], it follows, that the flow velocity component v_x presented in Figure 13, and lubricant dynamic viscosity distributions η across the gap height are not constant. We show the phenomenon of the human sweat dynamic viscosity η variations across the very thin layer between the human skin surface and tightly fitting sports dress surface.

The sweat dynamic viscosity distribution in the gap height direction is depicted on the right-hand side of Figure 13 and is assigned to the velocity distributions in across-section A, and B presented on the left side of the mentioned figure. We can see that the dynamic viscosity distribution in thin gap height direction, depends on the variations of velocity and shear rate distribution variations. Moreover, the sweat velocity and shear rate distribution variations in thin gap height direction influence the dynamic viscosity and hydrodynamic pressure distribution. In Figure 13 the hydrodynamic pressure quantity p is of order O (0.00150 MPa) with temperature values 310K < T < 312 K, lactic acid LA = 200 mg/100 ml sweat, training activity level TA = 3, wettability We = 40°, power hydrogen ion concentration pH = 5. Decrements in the flow velocity and shear rate values imply the liquid dynamic viscosity increases from 0.00003 Pas to 0.00300 Pas. However, if velocity attain values in zero neighborhood, then the viscosity tends only to approximate value 0.00299 Pas on the ground of measurements.

Figure 13 show, the sweat flow inside the presented thin layer between movable human skin's lower surface and movable tightly fitting sports dress material upper surface. Mentioned flow is not generated by the constant hydrodynamic pressure, only by the motion in two opposite directions of the lower skin and upper dress material surfaces.

The places in Figure 13 of maximum (minimum) values of the sweat velocity distribution in the gap height direction, i.e., in thin layer, have the minimum (maximum) values of the dynamic sweat

viscosity. The coinciding point of two charts A and B of the dynamic sweat viscosity in Figure 13 denotes the point in gap height direction with identical absolute values of sweat velocity in s sections A and B.

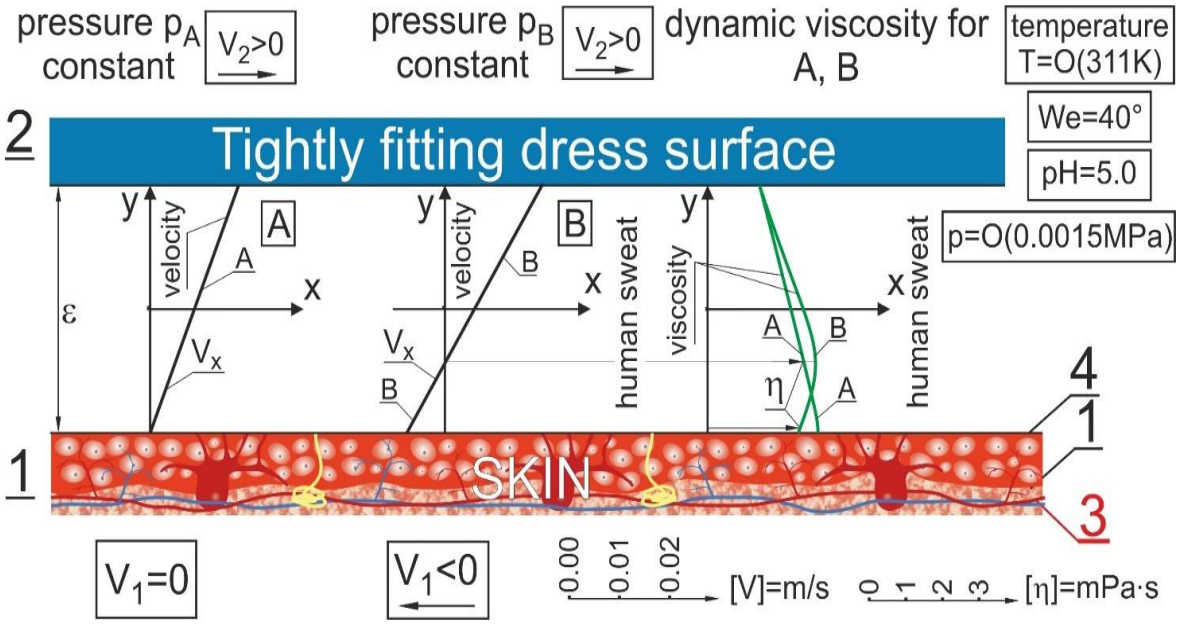

Figure 13 Determination of the dynamic viscosity η distribution across the thin sweat boundary layer in two sections A&B, between movable upper (2) sports dress surface and motionless lower skin surface in section A, and between movable upper dress surface (2) and movable lower skin surface (1) in opposite directions in section B. Both sections A and B are loaded with the constant pressure values. Notations: velocity component v_x with values V_1, V_2 on the lower and, upper surfaces, 1-epiderm, 2-sport dress material, 3-skin, 4-corneal layer.

5.3 Corollaries and Applications for Human Skin Lubrication

In this intersection are illustrated some lubrication phenomena for human skin. In particular case is considered the human sweat flow in the thin gap between two cooperating surfaces namely the human skin surface and tightly fitting dress material. It is evident, that the temperature differences between upper and lower mutually cooperating surfaces restricting the thin layer filled with sweat, have negligibly small influences on the dynamic viscosity variations. However the sweat velocity depended on important temperature gradients across the film thickness and hydrodynamic pressure is assigned to the largest values and variations of the sweat viscosity in the gap height direction. Hence, largest dynamic viscosity variations in gap height direction, influence the hydrodynamic pressure increases. After presented investigations had been proved the mutual connections between load carrying capacity and sweat velocity as well dynamic viscosity in gap height direction during the run, movement of human limbs and hydrodynamic skin lubrication. The one piece dress is presented in Figure 14a, 14b and 14c. And is labeled as Figures 9, 10, 11, 12.

Figure 14 One piece sport training tightly fitting dress: a) used for runner during the run, b) used for dancer, c) used during the skill in acrobatics for the athlete in professional sport.

The pressure and load carrying capacity obtained from hydrodynamic sweat lubrication can be implemented and used as the additionally, proper synergetic force during the finish run by the runner (Figure 14a), during the balance keeping for ballet dancer (Figure 14b) and during the skill in acrobatic gymnastics for the athlete in professional sport (Figure 14c).

During the motion in one piece training tightly fitting dress the sportsman gains the tangential friction forces which are steadily distributed on the all body surface. This fact increases fitness efficiency during the acrobatic feat and human Basal Metabolic Rate (BMR).

6. Non Published Results for Thin Synovial Liquid Cartilage Random Lubrication in Human Joint

This intersection presents recent progress in the knowledge concerning the stochastic theory of tribology hydrodynamic parameters for the real human hip joint spherical surfaces coated with

cartilage restricted deformed gap height. Based on experimental measurements and numerical solutions [36], the research concerns the influences of the random expectancy values of human hip joint gap height on the synovial fluid dynamic 3D variations [46-50].

Now some possible results are presented after applying the Wierzcholski summation and recurrence, numerical calculation [36] using devices and partial differential hydrodynamic equations presented in intersections 2.2 & 2.3. Numerical efforts have been preferred in the mentioned scientific domain of a new bio-medicine tribology and bio-lubrication problems of human joints.

First, we show in Figures 15abcde the hydrodynamic pressure distributions on the various rotational shapes of the human bone head and for dynamic viscosity variations across the film thickness in the human joint gap presented in Figure 2a, 3a, 13.

We obtain the following maximum pressure values: a) 0.15 MPa, b) 0.15 MPa, c) 0.12 MPa, d) 0.16 MPa, e) 0.17 MPa [31, 47]. Numerical calculations are performed for: Bone surface wettability We = 60°, power hydrogen ion concentration pH = 6, the concentration of collagen fibers $\delta_v = 4$, bio-liquid flow index n = 0.9. In this flow we have: dimensional collagen fibers concentration c_c = 50 000 mol/mm^3, bio-liquid dynamic viscosity η = O (0.24 Pas), interfacial energy γ = 3.0 mJ/m^2, temperature T = O (310 K).

The pressure values depicted on the cylindrical, spherical, parabolic, and conical bone surfaces of the human joint, are successfully obtained from the partial-integral, second-order, strong non-linear, modified Reynolds Equation, using UNR: Unit –Net- Region mega algorithm implemented by a new summation and recurrence methods described in the book [36]. According to the contemporary knowledge mentioned recurrence calculation methods are completely new and have not been initiated so far by any scientific center and in any sphere of tissue engineering.

The classical numerical solution of mentioned strong nonlinear Reynolds Equation often leads to the existence of more than two functions which are numerical solutions for pressure and an envelope of a family of surfaces which are presented mentioned functions as the solutions. In this situation we are finally not sure we have obtained the proper solution in numerical calculations. Mentioned solutions are likewise difficult to obtain entirely numerical, even when the methods are complemented by the new contemporary computer programs [36].

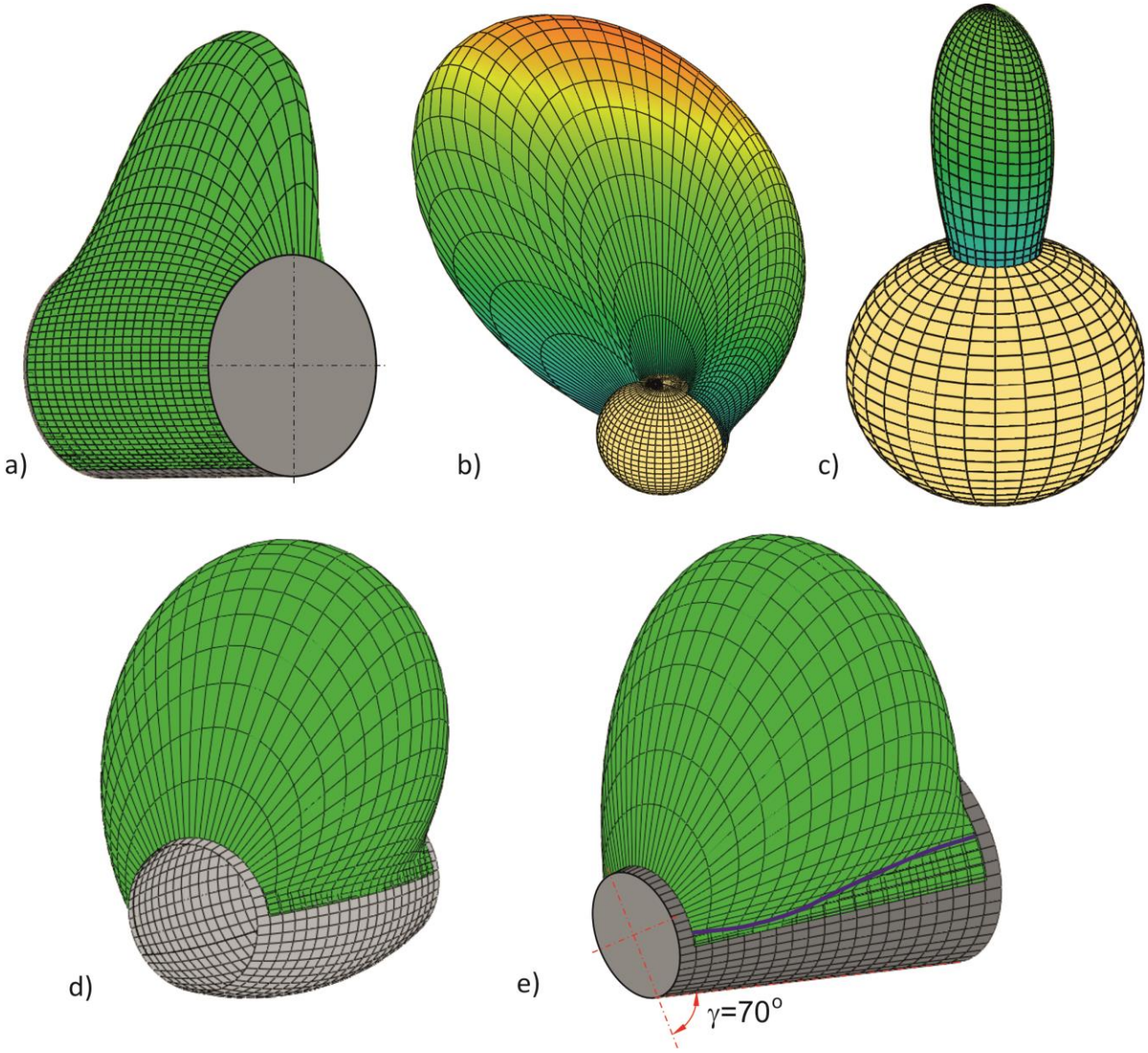

Figure 15 Bio-hydrodynamic pressure distributions on the human bone heads with various surface shapes and motion: a) cylindrical (radius 0.02 m) in rotation, b) spherical (radius 0.026 m) in rotation, c) spherical (radius 0.026 m) in squeezing, d) parabolic (radius 0.025 m) in rotation, e) conical (radius 0.02 m) in rotation.

7. Final Conclusions

7.1 Conclusions for Superficial Bio-liquid Layer Lubrication on the Living Tissue

During the tissue lubrication, the bio-liquid has apparent dynamic viscosity variations across the superficial layer height (thickness). After many experimental measurements and numerical computations, we obtained reality values of viscosity variations of about: 7% caused by the adhesion forces, 5% caused by the wettability of the living tissue restricted gap, 5% caused by the temperature gradients, 6% caused by the hydrogen ion concentration (pH) in bio-liquid, 10% caused by the shear rate and velocity during the flow.

7.2 Conclusions for Thin Bio-liquid Layer Lubrication Between Phospholipids Bilayer

By the computer calculations [36] we show a new extended description of influences of the various parameter, on the apparent dynamic viscosity variations and on the hydrodynamic pressure distribution in gap height direction across the bio-liquid layer between phospholipid bilayer. We obtain following variations of bio-liquid dynamic viscosity across the film thickness:

- 10% increases in dynamic viscosity, after 6% increments of the interfacial energy mJ/mK, in the gap height direction,
- 15% increases in dynamic viscosity, after 15% increments of the adhesion effects and increments of cartilage surface region A [m^2] coated by phospholipid molecules, in the gap height direction,
- 13% increases in dynamic viscosity after 12% decrements, of the shear rate in the gap height direction.

7.3 Conclusions for Thin Sweat Layer Lubrication Between Human Skin and Tightly Fitting Dress

The core of a new bio-nano-tribology research connected with the multidisciplinary scientific domains are realized by using experimental measurements and new contemporary numerical methods authenticated with the necessary electronic devices. In this intersection are presented some following new final conclusions for skin surfaces lubrication problems connected with human efficiency and health:

- Here are illustrated some following lubrication phenomena across the boundary sweat layer for dynamic viscosity variations of the sweat between human skin and tightly fitting dress surface:
  - small sweat velocity leads to the large sweat dynamic viscosity,
  - large sweat velocity leads to a small sweat dynamic viscosity.
- Training human capacity activity and dynamic sweat viscosity varies in the following form:
  - increases if lactic acid increases,
  - increases if power hydrogen ion concentration decreases from 7 to 4,
  - increases if the wettability of the dress surface material decreases.
- Even though, the temperature between upper and lower surfaces restricted the thin layer sweat, have negligibly small differences we have the following phenomena in gap height direction:
  - The human sweat velocity and its components depend on important temperature gradients across the film thickness. Such gradients are assigned to the largest variation values of the dynamic sweat viscosity in the gap height direction. Hence largest sweat dynamic viscosity variations in gap height direction, have important influence on the hydrodynamic pressure increases.
  - After presented investigations had been proved the mutual connections between human load carrying skin capacity and sweat velocity and dynamic viscosity variations in gap height direction during the hydrodynamic lubrication for human skin.

7.4 Conclusions for Thin Synovial Liquid Cartilage Random Lubrication in Human Joint

- The increments of the hip joint gap height ca. from 9 to 12 percent for PS (Phosphatidylserine) and from 15 to 19 percent for PC (Phosphatidylcholine) leads to the stochastic and expected 8 percent increases of the values of synovial fluid dynamic viscosity in comparison with the dynamic viscosity for joint gap height without random effects.
- By performed measurements follows, that during the rotation and squeezing, hydrodynamic lubrication, the random increments (decrements) of the joint gap height imply increases (decreases) of the synovial dynamic viscosity.
- Suppose the bio-liquid performs the rotation flow on the flexible cartilage. In that case, the dynamic viscosity of this liquid is large than the dynamic viscosity of the flow in the same rotation liquid flow but on the less flexible cartilage.
- Suppose the bio-liquid realizes the squeezing flow on the flexible cartilage. In that case, the dynamic viscosity of this liquid is less than the dynamic viscosity of the flow in the same squeezing liquid flow but on the less flexible cartilage.

8. Discussion

The presented experimental and numerical research illustrates the relationships and influences of the proper values of the dynamic viscosity of the human, biological, pharmacological liquids such as synovial liquids, sweat, saliva, and the proper therapy of these human liquids, on the human metabolism and skill. From the physiotherapeutic point the value of the abovementioned, human bio-liquid dynamic viscosity has a direct and indirect influence on the characteristic human skill and health parameters such as Body Mass Index (BMI), Basal Metabolic Rate (BMR), Metabolic Age (MA).

BMI denotes the body weight (KG) divided by the second power of the human height (in m). European have following values of BMI: 18 for underweight, 18-24.99 for optimum weight, 25.0-26.9 for the overweight first step, 27.0-29.9 for the overweight second step, 30.0-34.9 for obesity first step, 35.0-39.9 for obesity second step, 40.0-49.9 for obesity third step, and 50> over obesity. Mentioned values are not valid for Africans. BMR denotes the difference between total energy (in Kcal) and burned energy (in Kcal).

Acknowledgments

Acknowledge the WSG Bydgoszcz University, street Garbary 2, Bydgoszcz, Poland, particularly Prof. dr. Ryszard Maciołek from WSG University Bydgoszcz, that have technically supported this work, with fund provider. Author thanks for many discussions during the work preparation.

Author Contributions

Prof. Ph.D., D.Sc. Krzysztof Wierzcholski: Project development, Ph.D. Jacek Gospodarczyk: data developments, experimental measurements, numerical calculations

Competing Interests

The author has declared that no competing interests exist.

References

1. Kumar S, Kumar R, Singh S, Singh H, Kumar A, Goyal R, et al. A comprehensive study on minimum quantity lubrication. Mater Today. 2022; 56: 3078-3085.
2. Kumar S. Influence of processing conditions on the mechanical, tribological and fatigue performance of cold spray coating: A review. Surf Eng. 2022; 38:324-365.
3. Kumar S. Influence of processing conditions on the properties of thermal sprayed coating: A review. Surf Eng. 2022; 37: 1339-1372.
4. Kumar S, Mahajan A, Kumar S, Singh H. Friction stir welding: Types, merits & demerits, applications, process variables & effect of tool pin profile. Mater Today. 2022; 56: 3051-3057.
5. Kumar A, Sharma R, Kumar S, Verma P. A review on machining performance of AISI 304 steel. Mater Today. 2022; 56: 2945-2951.
6. Singh S, Kumar H, Kumar S, Chaitanya S. A systematic review on recent advancements in Abrasive Flow Machining (AFM). Mater Today. 2022; 56: 3108-3116.
7. Gadomski A, Bełdowski P, Rubi JM, Urbaniak W, Augé II WK, Santamarìa-Holek I, et al. Some conceptual thoughts toward nanoscale oriented friction in a model of articular cartilage. Math Biosci. 2013; 244: 188-200.
8. Scherge M, Gorb SN, Stone HA. Biological micro and nanotribology: Nature's solutions. Physics Today. 2002; 55.
9. Sandyk R. Therapeutic effects of alternating current pulsed electromagnetic fields in multiple sclerosis. J Altern Complement Med. 1997; 3: 365-386.
10. Pawlak Z, Urbaniak W, Hagner-Derengowska M, Hagner W. The probable explanation for the low friction of natural joints. Cell Biochem. Biophys. 2015; 71: 1615-1621.
11. Bagnato GL, Miceli G, Marino N, Sciortino D, Bagnato GF. Pulsed electromagnetic fields in knee osteoarthritis: A double blind, placebo-controlled, randomized clinical trial. Rheumatology. 2016;55: 755-762.
12. Cunha FR, Rosa AP, Dias NJ. Rheology of a very dilute magnetic suspensions with micro-structures and nanoparticles. J. M. Magn. Mater. 2016; 397: 266-274.
13. Marra J, Israelachvili J. Direct measurements of forces between phosphatidylcholine and phosphatidylethanolamine bilayers in aqueous electrolyte solutions. Biochemistry. 1985; 24: 4608-4618.
14. Bhushan B. Nanotribology and nanomechanics of MEMS/NEMS and BioMEMS/BioNEMS materials and devices. Microelectron Eng. 2007; 84: 387-412.
15. Ziegler B, Wierzcholski K, Miszczak A. Test stand in University of Applied Science Giessen for friction forces measurements in slide bearing using the acoustic emission method. J Kones Powertrain Transport. 2008; 15: 591-595.
16. Chagnon G, Rebouah M, Favier D. Hyper-elastic energy densities for soft biological tissues: A review. J Elast. 2015; 120: 129-160.
17. Wierzcholski K. Nanotribology impact of run-walk, electromagnetic-hydrodynamic human joint and skin lubrication on the slimming and metabolic process. Ann. Nanosci. Nanotechnol. 2017; 1: 1-8. Available from: https://www.remedypublications.com/open-access/nanotribology-impact-of-run-walk-electro-magnetic-hydrodynamic-human-joint-and-skin-lubrication-on-the-slimming-and-metabolic-process-657.pdf.
18. Bhushan B. Handbook of micro/nano-tribology.2nd ed. Boca Raton: CRC Press; 1999.

19. Wierzcholski K, Gospodarczyk J. On random expected values variations of tribology parameters in human hip joints surfaces. Tribologia. 2021; 297: 45-56. doi: 10.5604/01.3001.0015.6898.
20. Wierzcholski K, Maciołek R. A new contribution in stochastic hydrodynamic lubrication for arbitrary bio-surfaces. Tribologia. 2020; 3: 63-76. doi: 10.5604/01.3001.0014.4766.
21. Wierzcholski K, Gospodarczyk J. Human joint and skin surfaces random lubrication implemented by run in electromagnetic and acoustic emission field. Determ. Nanomed. Nanotechnol. 2022; 2: 1-5. DNN.MS.ID.000546. Available from: http://crimsonpublishers.com/dnn/pdf/DNN.000546.pdf.
22. Andersen OS, Koeppe RE. Bilayer thickness and membrane protein function: An energetic perspective. Annu Rev Biophys Biomol Struct. 2007; 36: 107-130.
23. Schwarz IM, Hills BA. Synovial surfactant: Lamellar bodies in type B synoviocytes and proteolipid in synovial fluid and the articular lining. Br J Rheumatol. 1966; 35: 821-827.
24. Hills BA. Boundary lubrication in vivo. J Eng Med. 2000; 214: 83-94.
25. Hills BA. Oligolamellar lubrication of joint by surface active phospholipid. J Reumatol. 1989; 16: 82-91.
26. EMS muscle stimulator [Internet]. Available from: https://www.leaflifetech.com/.
27. Wierzcholski K, Miszczak A, Cwanek J. Relations between viscosity of synovial fluid, gap height and angular velocity, young modulus of cartilage. Mech Med. 2002; 6: 201-207.
28. Cwanek J, Wierzcholski K. Measurements of head surfaces of endoprosthesis. Insycont 2006: 7th International symposium energy and environmental aspects of tribology; 2006 September 14th-16th; Cracow, Poland.
29. Tanita. HealthPlanet [Internet]. Available from: https://www.tanita.com/en/.
30. Skrobacki A, Veith J. Sweat components and its variations. Lab. Diagnosis. Medical Academy Warsaw. 1967; 3: 11-13. Available from: https://agro.icm.edu.pl.
31. Wierzcholski K. A new progress in random hydrodynamic lubrication for movable non-rotational curvilinear biosurfaces with phospholipid bilayers. Recent Prog Mater. 2021; 3: 023.
32. Czaban A, Frycz M, Horak W. Effect of the magnetic particles concentration on the ferro-oil's dynamic viscosity in presence of an external magnetic field in the aspect of temperature changes. J Kones Powertrain Transport. 2013; 20: 55-60.
33. Truckenbrodt E. Strömungsmechanik. Berlin: Springer; 1986.
34. Wierzcholski K, Miszczak A. Mathematical principles and methods of biological surface lubrication with phospholipids bilayers. Biosystems. 2019; 178: 32-40.
35. Wierzcholski K. The metabolic probabilistic effects of e-m hydrodynamic lubrication for synovial fluid and sweat in the human joint and on the skin, in monograph: Multiscale (Loco)motion, ed by A.Gadomski, UTP Univ. Bydgoszcz. 2019; 81-119. ISBN 978-83-65603-96-8. Available from: http://www.wu.utp.edu.pl.
36. Wierzcholski K. Applications of summation and recurrence equations. Saarbrücken, Lambert, Academic Publishing Company, Omni-scriptum GmbH & co. 2014; 1-359. ISBN 978-3-659-57184-8. Available from: http://www.lap-publishing.com/; https://www.amazon.pl/Applications-Summation-Recurrence-Equations-Wierzcholski/dp/3659571849.
37. Johnston GJ, Wayte R, Spikes HA. The measurement and study of very thin lubricant films in concentrated contacts. Tribol Trans. 1991; 34: 187-194. doi: 10.1080/10402009108982026.

38. Wierzcholski K, Gospodarczyk J. On important meaning of bio-fluid dynamic viscosity variations in the lubrication flows. Tribologia. 2022; 1: 83-95. doi: 10.5604/01.3001.0015.8987.
39. Szeri AZ. Fluid film lubrication. Cambridge: Cambridge University Press; 1998.
40. Kasolang S, Dwyer-Joyce RS. Viscosity measurement in thin lubricant films using shear ultrasonic reflection. J. Eng. Tribology 2008; 222: 423-429.
41. Zernecke R, Kleemann AM, Haegler K, Albrecht J, Vollmer B, Linn J, at al. Chemosensory properties of human sweat. Chem Senses. 2010; 35: 101-108.
42. Mehrdad A, Shekaari H, Noorani N. Density, speed of sound, viscosity and conductivity of lactic acid in the aqueous solutions of polyethylene glycol at different temperatures. J Mol Liq. 2018; 255: 454-461. doi: 10.1016/j.molliq.2018.01.184.
43. Groot W, Van Krieken J, Sliekersl O, De Vos S. Production and purification of lactic acid and lactide. Lactic Acid.2010; 1-18. doi: 10.1002/9781119767480.ch1.
44. Starr JN, Westhoff G. Lactic Acid. 2014; 1-8. doi: 10.1002/14356007.a15_097.pub3.
45. Halonen S, Kangas T, Haataja M, Lassi U. Urea-water-solution properties: Density, viscosity, and surface tension in an under-saturated solution. Emiss Control Sci Technol. 2017; 3: 161-170. doi: 10.1007/s40825-016-0051-1.
46. Wierzcholski K, Gospodarczyk J. The metabolic process after lubrication of human joint and skin surfaces. Clinical Research Notes, Auctores Publishing. 2022; 3: 1-11.
47. Wierzcholski K, Miszczak A. Estimation of random bio-hydrodynamic lubrication parameters for joints with phospholipid bilayers. Bull Pol Acad Sci Technical Sci. 2021; 69: e135834. doi: 10.24425/bpasts.2021.135834. Available from: http://www.journals.pan.pl.
48. Cwanek J. The usability of the surface geometry parameters for the evaluation of the artificial hip joint wear. Rzeszów: Rzeszów University Press; 2009.
49. Mow VC, Ratcliff A, Woo S. Biomechanics of diarthrodial joints. New York: Springer; 1990.
50. Wierzcholski K. Time depended human hip joint lubrication for periodic motion with stochastic asymmetric density function. Acta Bioeng Biomech. 2014; 16: 83-97. Available from: http://www.actabio.pwr.wroc.pl.